

Thermal Conductivity of Cadmium and Cadmium-Alloy Crystals*

R. Bogaard[†] and A. N. Gerritsen

Department of Physics, Purdue University, Lafayette, Indiana 47907

(Received 27 March 1970)

The intrinsic thermal resistivities W_i of pure Cd and of Cd-Zn single crystals with residual-resistance ratios in the range $5 \times 10^4 - 570$ (Zn content up to 0.56 at.%) were determined for both hexagonal and basal orientations in the temperature range $3 < T < 100$ K. One Cd-Sn crystal (0.14 at.% Sn) was measured in the basal orientation. The data are represented by $W_i \propto T^n$. In the case of pure Cd, $n=2$ for $T < 3.5$ K, whereas for the most impure alloy, $n=2$ for $T < 13$ K. For temperatures above the $n=2$ region, n was found to be as large as 4.5 in the interval $4 < T < 7$ K in the case of the purest crystal. The known rapid change of the specific-heat Debye Θ does not explain the large n . This indicates a small to negligible interaction between the electrons and transverse phonons. The region where $n > 2$ is, in general, in the temperature range where phonon scattering outweighs impurity scattering. It is suggested that because of the particular shape of the Fermi surface, umklapp processes may be important in and above the temperature range where n is large.

INTRODUCTION

It has been known for some time that the low-temperature electronic intrinsic thermal resistivity of cadmium deviates from the usual T^2 behavior. Rosenberg's¹ data on a pure single crystal indicate two distinct regions of quadratic behavior separated by a transition region having a stronger temperature dependence. An explanation was sought in terms of drastic changes in the phonon spectrum at low temperatures. Measurements of the electrical resistivity² of pure single crystals of cadmium as a function of temperature have not indicated an anomalous behavior. Therefore the explanation of the behavior of the thermal resistivity appears to require a more detailed description of the electron-phonon interaction than the general phonon-behavior argument put forward previously.¹

There is now evidence for more specialized effects in the hexagonal metals. Observations have been made of phonon scattering effects³ in magnesium and, more recently, electron scattering effects⁴⁻⁶ in cadmium. The phonon effects in magnesium appeared in the electrical resistivity as deviations from Matthiessen's rule for a variety of impurities. A theoretical treatment⁷ showed that a variety of second-order effects may result from the interaction of an impurity with the electron and phonon systems. The electron scattering effects in cadmium appeared in the galvanomagnetic properties as a specialized form of scattering, strongly dependent upon certain features of the Fermi surface.⁵

It seemed justifiable to systematically reinvestigate the electron thermal resistivity of cadmium, that is now available in slightly purer form, with the hope to contribute to a classification of the respective roles of the phonon and electron systems.

Whereas the results given in the literature indicate a strong influence of impurities on the electron-phonon scattering term in the temperature dependence of the thermal resistance, several crystals having controlled amounts of zinc impurities have also been investigated.

The results show that besides contributing to the normal impurity scattering the small amounts of zinc impurities indeed do affect the temperature dependence of the electron-phonon scattering term in a consistent and fundamental manner. Yet, the interaction among the different scattering processes and, in particular, the complexity of the Fermi surface of cadmium make, at present, only qualitative explanations of the observed phenomena possible.

EXPERIMENTAL METHOD

a. Sample preparation. Most samples were cut from a commercially obtained⁸ pure single crystal of cadmium for which $r_{1.4}$ (the ratio of room-temperature electrical resistance to that at 1.4 K) was of the order of 5×10^4 for a sample oriented parallel to the hexagonal axis.

The impurities alloyed with the cadmium were either zinc or tin. Zinc was used because its valency is the same as that for cadmium and it crystallizes in an elongated hexagonal structure. The one alloy with tin was made to check whether the effect of a change in the electron/atom ratio on the electron thermal conductivity could be observed.

The diffusion method used for alloying a pure single-crystal sample with zinc or tin has been described elsewhere.⁴ The process began with electroplating the solute element onto a pure single-crystal cadmium blank, followed by a diffusion at 200 °C lasting 4-7 days. After etching off surface residue, the sample was homogenized for a week

at 200 °C.

As a measure of the homogeneity of the alloys prepared in this manner, the value of $r_{4,2}$ was found to change by no more than 20% when the sample width was etched down from 1.2 to 0.3 mm.

In addition to the samples alloyed as described above, one commercially alloyed single crystal⁹ was obtained from which two samples Cd-ZnA2 and Cd-ZnC2 were cut. A or C before the sample number indicates the direction of the length and the heat flow perpendicular or parallel to the C axis. A spectrographic analysis¹⁰ of the pure Cd and the alloy samples was made after all measurement series were finished. The results of the analysis are listed in Tables I and II.

In preparation for the thermal-resistance measurements, the samples were shaped and planed with a spark cutter.¹¹ Two side arms were left on one side of the sample for attaching thermometers. After the final planing operation, at least 0.1 mm of material was etched off to remove sparking damage. Typical final dimensions were 2.5 cm × 1.5 mm × 1.5 mm with the side arms 0.3 mm thick. The samples were annealed at 200 °C for 6 h before they were mounted in the cryostat.

b. Cryostat and measurement. A cryostat of standard design with the sample mounted in a vacuum-isolated can was used. Its construction is described elsewhere.¹² The thermometers were encapsulated germanium crystals that were obtained commercially.¹³ Thermometer voltages were measured with a 5-dial Diesselhorst compensator¹⁴ along with a galvanometer¹⁵ as null detector. The maximum sensitivity of the system was 10^{-7} V. The heater power was calculated from measured values of voltage and current, using a millivolt potentiometer.¹⁶ The simple steady-heat-flow method was used. The temperature difference between the two thermometers was calculated from the determination of the resistance ratio between them. The method is similar to that reported for two Pt resistance thermometers.¹⁷

One of the two thermometers used for the deter-

TABLE I. Mass spectrographic analysis of Cd as provided by Battelle Memorial Institute.

Element	ppmw	Element	ppmw
Li	3	Ag	<0.6
C	3	In	<3
N	2	Sn	<5
O	2	Te	<2
Cl	4	Ta	≤5
K	2	Au	<2
Ca	7	Ba	<0.5
Ti	0.6	W	<0.6
Cr	0.2	Tl	<0.7
		Th	<0.7

TABLE II. Atomic-absorption spectroscopic analysis of Cd alloys as provided by Battelle Memorial Institute.

Sample code	Resistance ratio	Concentration (at. %)	
		Zn	Sn
Cd-AnA1	570	0.56	
Cd-ZnC1	3100	0.084	
Cd-ZnA3	2700	0.095	
Cd-SnA1	7700		0.14
Cd-ZnA2	1.9×10^4	0.011	
Cd-ZnC2	1.8×10^4		

mination of ΔT was calibrated against a thermometer for which the calibration was supplied by the manufacturer.¹³ The given accuracy varied between 0.1 and 0.2% depending on the specific temperature range. The values of ΔT were, in general, restricted to 1% of T , and the relative uncertainty in ΔT is estimated at 1.5%. Taking into account, also, the uncertainties in the determination of the heat flow T and the form factor, it is estimated that the uncertainties are 2 and 5% for the measured resistance and resistivity, respectively.

EXPERIMENTAL RESULTS

At temperatures above approximately 50 K, where the electron-phonon scattering is temperature independent, all samples approach a thermal conductivity on the order of $1 \text{ W cm}^{-1} \text{ K}^{-1}$. This has been illustrated for a few samples in Fig. 1, where the thermal conductivity κ has been plotted for the pure-Cd and the Cd-Zn alloys as a function of temperature. The curves in Figs. 1(a)–1(d) illustrate the changes of the $\kappa(T)$ relations from different causes. In parts (a) and (b) the effect of increasing

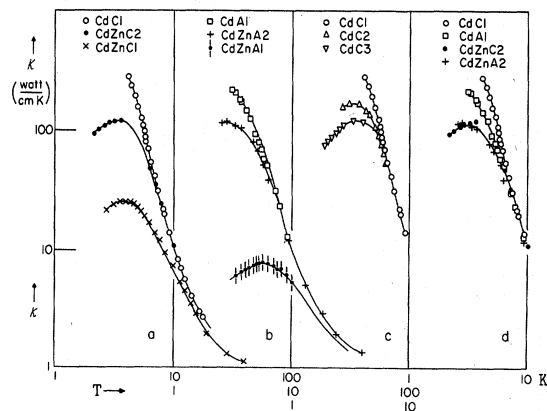


FIG. 1. Measured conductivities for several crystals with heat flow parallel (C) or perpendicular (A) to the hexagonal axis. Illustrated are the effects of increasing solute [parts (a) and (b)], size effect [part (c)] and the diminishing effect of anisotropy with increasing amounts of solute [part (d)].

Zn concentration is demonstrated for the heat flow parallel (a) and perpendicular (b) to the hexagonal axis. Part (c) represents the effect of the reduction of the cross section of a sample of pure Cd on the maximum in the $\kappa(T)$ curves, and in part (d) is illustrated the anisotropy for two pure-Cd crystals and two alloys of different orientation but each pair having the same purity. The effective purity of the samples is given in Table III in terms of the residual-resistance ratio $r_{1.4}$, which is the resistance ratio between room temperature and 1.4 K. For the pure samples this ratio may decrease as much as a factor of 2 from 4 to 1.4 K.⁴ The usual features are represented in these curves; an increase in the amount of solute decreases the magnitude of the maximum in conductivity and shifts it to a higher temperature, and the size effect is similar to that of increasing solute amount. It is also clear that with increasing temperature the effects of the impurity diminish and that impurities may obscure the crystal anisotropy even at low temperatures.

Deviations from this seemingly normal behavior become evident when the electronic part of the conductivity is considered. This will be discussed in terms of the properties of the electronic (W_m) or intrinsic (W_i) thermal resistivity.

In the region where the lattice conductivity is negligibly small, the usual expression¹⁸ for the measured electronic thermal resistivity W_m of a metal at low temperatures is

$$W_m = W_0 + W_i = \beta/T + aT^n. \quad (1)$$

Here β is the impurity scattering parameter and $W_i = aT^n$ is the electron-phonon scattering resistivity.

In order to determine W_i , the conventional technique of assuming $n = 2$ and plotting $W_m T$ vs T^3 was used. Such a graph is shown in Fig. 2 for a pure-Cd sample and a Cd-Zn alloy. The orientations

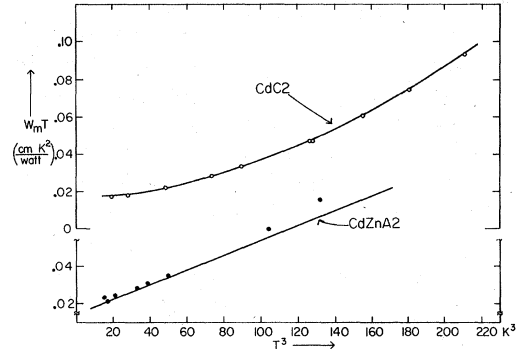


FIG. 2. $W_m T$ vs T^3 for pure Cd (Cd C2) and a Cd-Zn alloy (Cd-Zn A2).

are, respectively, parallel to and perpendicular to the hexagonal axis. It is seen that the data do not represent a straight line in the case of the pure Cd, but that for Cd-Zn a straight line below 4 K allows a determination of β . For $T > 4$ K the data for Cd-Zn deviate markedly toward larger ordinate values. This indicates a $n > 2$.

The failure of the assumption $n = 2$ makes the determination of W_0 difficult, in particular, for pure Cd. For these samples, plots of $W_m T$ vs T^4 , T^5 , and T^6 were used to obtain converging estimates of β . If a nonobserved region, where $n = 2$, were to exist for $T \rightarrow 0$ K below $T \approx 3$ K, the estimated values of β for those samples would be larger than the true values. However, in view of the small magnitude of β , this difference would not be large enough to significantly affect either the magnitude or the temperature dependence of W_i for those temperatures where $W_i > W_0$.

The β values so obtained vary linearly with $1/r$. Using the value for the Zn concentration, $c = 0.56$ at % for sample Cd-ZnA1 as the most reliable, an estimate for the electrical and thermal atomic-

TABLE III. Sample data for Cd and alloy crystals; heat flow parallel (C) or perpendicular (A) to the hexagonal axis.

Sample	$r_{1.4}$	Width (mm)	β (cm K ² /W)	$a_{n=2}$ (10 ⁻⁵ cm/WK)	Temperature range (K)	n	Temperature range (K)
Cd C1	$\sim 5 \times 10^4$	1.90	~ 0.006	4.5	4-7
Cd C2	$\sim 5 \times 10^4$	0.70	0.016	4.1	4-6
Cd C3	$\sim 5 \times 10^4$	0.45	0.026	17	2.5-3.5
Cd-Zn C1	3.1×10^3	1.13	0.115	3.0	3-7
Cd-Zn C2	1.8×10^4	1.03	0.020	21	2.5-3.6	3.5	4-10
Cd A1	$\sim 5 \times 10^4$	2.15	~ 0.005	4.1	4-7
Cd-Zn A1	5.7×10^2	1.00	0.50	2.2	3-13
Cd-Zn A2	1.9×10^4	1.12	0.015	40	2.5-3.7	3.1	5-10
Cd-Zn A3	2.7×10^3	1.16	0.123	75	2.5-5	2.8	6-10
Cd-Sn A1	7.7×10^3	1.04	0.037	53	2.5-5	2.9	6-11
Cd R ^a	0.025	35	2-4
				127	9-14		

^aHeat flow 40° off hexagonal axis; see Ref. 1.

resistivity increases can be obtained. Since

$$1/r = [\rho_{cd}(4) + c\delta\rho] / [\rho_{cd}(300) + c\delta\rho],$$

it follows that the atomic-resistivity increase $\delta\rho$ for Zn in Cd is of the order $3 \times 10^{-3} \rho_{cd}(273)/\text{at. \%}$. From the linear relation $\beta(1/r)$, the estimate $\delta\beta = 0.95 \text{ cm K}^2 \text{ W}^{-1}/\text{at. \%}$ is found. This implies that for 1 at. % Zn at 100 K the solute contributes at most 1% to the thermal resistance.

Data for all samples were plotted as $\log_{10} W_i$ vs $\log_{10} T$. In Figs. 3 and 4 are shown data for samples oriented with the heat flow parallel to the hexagonal axis.¹⁹ Figure 5 shows data for samples with the perpendicular orientation. It is seen that, in general, $n > 2$ below approximately 10 K and that, depending upon the impurity content, n may equal 2 at a still lower temperature range. Above 10 K the curves reflect the approach to $W_{i\infty}$, the temperature-independent resistivity at high temperatures.

Also shown on Fig. 3 is Rosenberg's sample¹ indicated by CdR. The orientation of this sample was reported to be tilted 40° with respect to the hexagonal axis. (The impurity parameter β is near that of our sample Cd-Zn C2.) It is seen that the data for CdR show the same character as those exhibited by the present data. It was reported¹ that for CdR a second region with $n = 2$ was observed for $9 < T < 14 \text{ K}$. The present results contain more

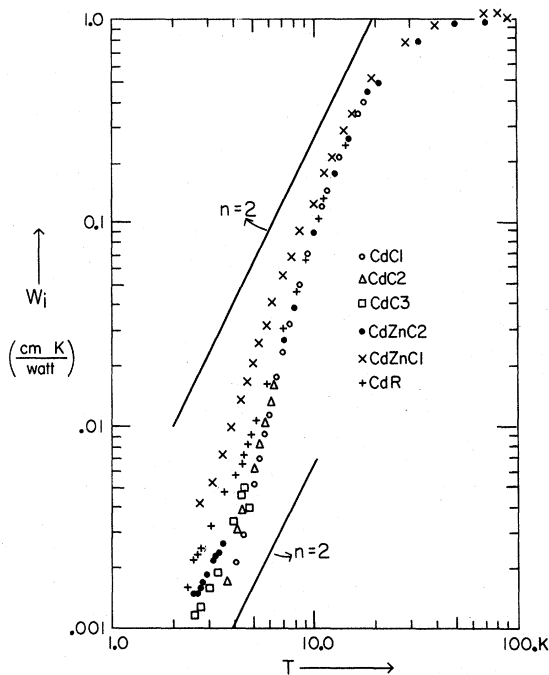


FIG. 3. Intrinsic thermal resistivity W_i plotted against the temperature for heat flow parallel to the hexagonal axis.

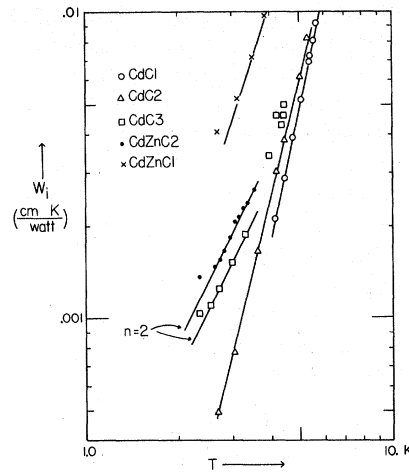


FIG. 4. Intrinsic thermal resistivity W_i plotted against the temperature for heat flow parallel to the hexagonal axis for temperatures below 10 K.

data in this region and do not show such behavior.

In Table III are given several parameters which characterize all the samples measured. The orientation is given as the sample length being parallel or perpendicular to the hexagonal axis. The phonon scattering parameter $a_{n=2}$ was obtained from the indicated temperature ranges where $W_i \propto T^2$. Apart from differences due to orientation, the a values in the present investigation are of the same order as those reported by other authors.¹

Samples Cd C2 and Cd C3 were etched versions

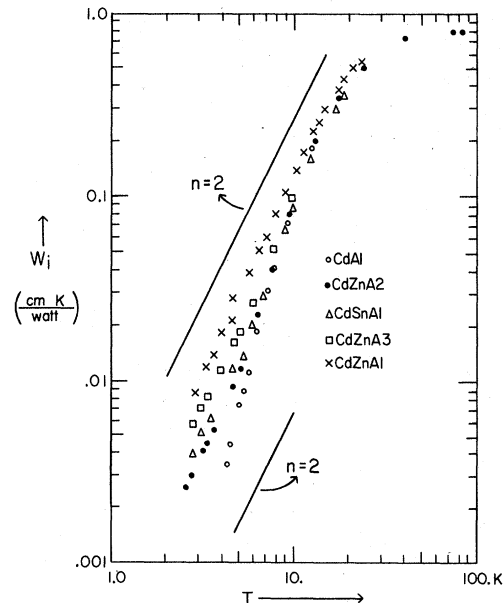


FIG. 5. Intrinsic thermal resistivity W_i plotted against the temperature for heat flow perpendicular to the hexagonal axis.

of CdC1, thinned down to permit an extension of that data to $T < 3$ K. Measurements on the size effects in the electrical resistivity of Cd have shown²⁰ that, assuming the Wiedemann-Franz (WF) ratio holds, an increase in β by factors of 2 and 3 could be expected for CdC2 and CdC3, respectively. In the present case, the measured increases in β , from 0.006 cm²/W to 0.016 and 0.026 cm²/W, respectively, indicate that considerable strain was present for CdC3. The increases in W_i are, therefore, a combination of size effect and strain. Size-effect measurements²¹ on indium have shown that the WF law does hold for a β dominated by boundary scattering. Furthermore, the size effect increases the magnitude of W_i but does not change its temperature dependence. This is similar to the effect of impurities.

It is worth noting (Fig. 5) that in contrast with the Hall properties⁴ an increase of the electron/atom ratio (Cd-Sn alloy) does not markedly affect the thermal behavior.

From the data it follows also that the ratio between the intrinsic resistivities parallel and perpendicular to the hexagonal axis varies with temperature. In Fig. 6 the ratios $W_{i\parallel}/W_{i\perp}$ are plotted against temperature for three pairs of samples having approximately equal β values (see Table III) but different orientation. The ratios are similar for the impure pairs of order 0.5 at 4 K, increasing to 1.2 at 30 K, and remaining constant at higher temperatures. The ratio seems to be rather insensitive to the amount of impurities. The plateau occurring just above 10 K could be an indication of two different effects of the anisotropy on W_i . On the other hand, the shape of the curve is certainly influenced by the experimental arrangement that does not allow the determination of $W_{i\parallel}$ and $W_{i\perp}$ at

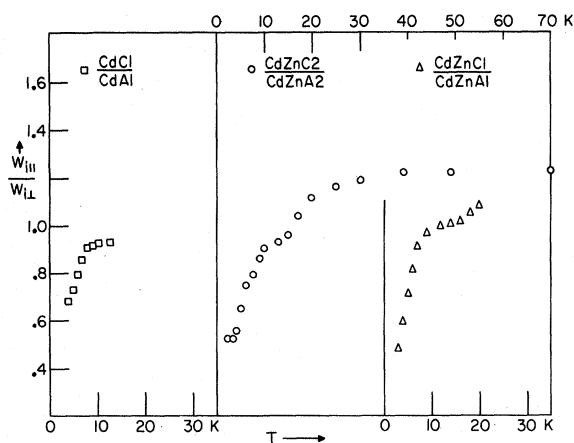


FIG. 6. Thermal anisotropy plotted as the ratio between the intrinsic resistivity parallel ($W_{i\parallel}$) and perpendicular ($W_{i\perp}$) to the hexagonal axis for three pairs of samples.

the same sample.

DISCUSSION

The results for the intrinsic thermal conductivity will be discussed first in terms of the observed changes in the Debye Θ and second in terms of possible electron scattering processes.

a. Correlation with specific heat. The marked change in n observed for most of the samples occurs at temperatures near which the lattice specific heat of pure Cd begins to deviate strongly from a Debye-like behavior. The most recent measurements²² in the range 1–4 K indicate that the Debye Θ decreases from 205 K at 1 K to 175 K at 4 K. Older measurements^{23,24} show that Θ begins to decrease from 190 K at 3 K to a minimum of 124 K at 10 K, followed by a much slower increase.

One is inclined to correlate¹ the thermal resistivity data with Θ through the well-known expression¹⁸

$$W_i \propto W_{i\infty} T^2 / \Theta^2. \quad (2)$$

Figure 7 is a plot of $W_i/(T/\Theta)^2$ vs T for samples with parallel and perpendicular orientations. The Θ values for $T < 3$ K are taken from Ref. 22, those for $3 < T < 5$ K are an average of the data from Refs. 22 and 23, whereas for $5 < T < 25$ K the Θ values are taken from Refs. 23 and 24. The same $\Theta(T)$ values were used for all samples although the change in Θ with impurity content is not known. One would normally, for these large dilutions, not expect this variation to be large enough to significantly affect the curves of Fig. 7.

It is seen that (2) is not satisfied. First of all, if (2) were to hold one would expect for each sample the ordinate to be, in first order, a constant for the temperature range considered. This seems to be so for the alloy Cd-ZnA1 ($r = 570$) above 7 K, and above 15 K for Cd-ZnC1 ($r = 3.1 \times 10^3$). With decreasing Zn concentration the departure from being constant becomes more marked: For the pure sample, the ordinate reaches a dip of more than a factor of 4. Below 7 K the expression (2) does not seem to be satisfied even for those samples for which, in the low-temperature range, $W_i \propto T^2$. It is clear that at least for samples of high purity ($r \geq 10^4$), the general relation (2) is not satisfied for $T < 25$ K. This would mean that the intrinsic thermal conductivity has no simple connection to changes in Θ , that is to the non-Debye character of the phonon spectrum. Since $\Theta(T)$ has been found²⁵ to pertain mainly to the transverse phonons, the failure of (2) implies that the scattering between electrons and transverse phonons is small indeed.¹⁸

b. Comparison with electrical resistivity. The intrinsic electrical resistivity ρ_i of a pure single-

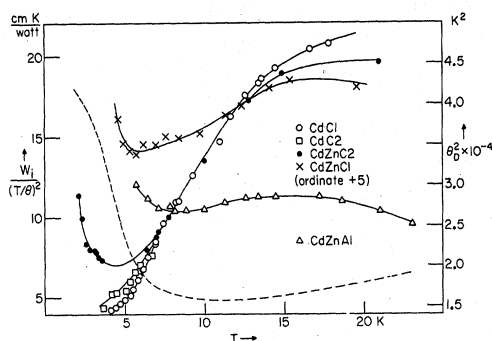


FIG. 7. Plot of $W_i/(T/\theta)^2$ vs T for a few samples with parallel orientation and for sample Cd-ZnA1. The dotted line represents Θ^2 vs T .

crystal Cd has been reported² to follow the usual T^5 behavior, up to about 14 K. Measurements of our sample CdA1 indicated a T^5 behavior up to 9 K. However, these measurements were carried out only with temperatures determined by the vapor pressures of helium and hydrogen liquids. Solid hydrogen was also used in our experiment in order to make measurements at $T \approx 9$ K. Therefore, the electrical-resistivity-temperature relation is not very well established for $4.2 < T < 9$ K.

Nevertheless, the intrinsic thermal and electrical resistivities were compared through their WF ratio $L_i = \rho_i/W_i T$. Figure 8 shows a plot of L_i/L_0 vs T for a pure sample (CdA1) and two alloys (Cd-ZnA1 and Cd-ZnA3), all in the perpendicular direction. Here L_0 is the Sommerfeld value of the Lorenz parameter. Estimated experimental uncertainties are indicated by vertical bars.

The primes shown on the 14 and 20 K points plotted for CdA1 indicate that the W_i values had not actually been measured. Instead, the measured values W_i for the dilute alloy Cd-ZnA2 were used to compute L_i . For Cd-ZnA2, the value of $r_{1,4}$ is less than that of CdA1 by a factor of 2.6. Since, on the other hand, the difference in W_i for the corresponding samples in the parallel orientation is not more than approximately 5%, an uncertainty of this order was included in the error bars shown.

It is seen that the curve for the pure material is rather flat ($L_i/L_0 = 0.5 \pm 0.1$) for all temperatures plotted, and those for the alloy curves have decreasing L_i/L_0 values at the lowest temperatures. The flatness indicates a certain similarity in the sensitivities of the two resistivities to scattering events. The inelastic nature of an electron-phonon scattering means that, in the case of the thermal resistivity, a single event is sufficient to remove the excess energy acquired from the temperature gradient. For the electrical resistivity, on the other hand, several small-angle scattering events may be required to move an electron around the

Fermi surface and thereby to remove the excess momentum picked up from the electric field. In other words, the effective relaxation time for the electrical resistivity may be several times larger than that of the thermal resistivity, depending upon the scattering angle. In terms of L_i/L_0 , a value of $L_i/L_0 = 1$ would mean that the two relaxation times were the same. The fact that the measured $L_i/L_0 \approx 0.5$ would indicate, within the frame of these simple considerations, that the relaxation time for the electrical resistivity is a few times larger than that for the thermal resistivity.

The similarity, in particular for the purest samples between the electrical and thermal conductivity as illustrated by the WF coefficient, leads to a consideration of those effects that are known to cause deviations from the Matthiessen rule and deviations from the T^5 temperature dependency for the electrical resistivity. Such deviations are, in general, second-order effects but their physical origin does, in principle, not exclude the possibility for deviations of larger magnitude in the $W_i(T)$ relations to occur. It will be shown that they seem to be inconsistent with the present data.

Assuming that the T^2 behavior is invalidated by an extra scattering process, it is most obvious to reconsider in (1) the simple additivity of W_0 and W_i . The well-known failure of this rule has been investigated by several authors and is most predominant in the electrical and thermal transport properties when impurity and intrinsic resistivities are of the same order. Attempts to add to (1) a mixing term in analogy with the problem in residual electrical resistance²⁶

$$W_{10} = k W_i W_0 / (l W_0 + m W_i),$$

with k , l , m constants of the order 1, have been very successful in the case of copper and aluminum alloys,²⁷ where deviations from the T^2 rule could be made to fit consistently a $W_i(T)$ relation for the base metal that remained the same for its alloys. In the present case, however, it seems that

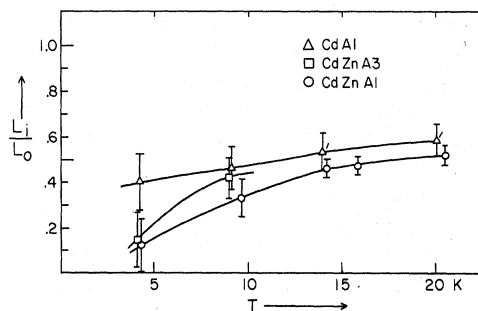


FIG. 8. Plot of the Lorenz parameter L_i relative to its Sommerfeld value L_0 vs T for three samples.

$W_i \propto T^2$ precisely in the temperature range where W_i and W_0 are comparable. For the pure Cd C1 and Cd C2 samples, $W_i \approx W_0$ at the lower end of the deviation range; for Cd C3 it is at the start of the lower T^2 branch. For Cd-Zn C2, $W_i \approx W_0$ well in the $n=2$ range, but for Cd-Zn C1 (for which β is 5 times larger), $W_0 \approx W_i$ in the upper third of the $n > 2$ range. In the case of the samples cut in the basal direction, $W_0 \approx W_i$ in the $n=2$ range for each sample investigated.

Rather recently Kagan and co-workers⁷ explained qualitatively large deviations from the Matthiessen rule that were found in a number of electrical resistance results, among others, in Mg-based alloys.³ They introduced different modes of non-elastic electron-phonon scattering, leading to terms in T^2 and T^5 that could account for the observed temperature variations (of order 20%) in the zero-degree residual resistance. These terms were most effective for $40 < T < 100$ K. For Mg-alloy crystals having approximately the same residual-resistance ratios, the intrinsic thermal resistance varied¹² as T^2 with deviations occurring only at temperatures below 4 K, in agreement with earlier published¹⁸ results for polycrystalline material. This observation more or less excludes the interesting idea of mixing of phonon modes⁷ as a possible explanation for the present results. The examination of these scattering phenomena does not seem to lead to a description of the present results.

c. Umklapp scattering as a possible explanation. A minimum in the $L_i(T)$ curve is attributed to one-velocity scattering being dominant at low temperatures. This type of scattering ("vertical"; the electron loses its kinetic energy without changing its position on the Fermi surface^{18,28}) is most drastic in the increase of thermal resistance relative to the scattering over the Fermi surface that accounts for the electrical resistance. Such a minimum in L_i does not occur for cubic metals for which the Fermi surface touches the boundary of the Brillouin zone. If, in these cases, umklapp scattering is taken into account in the theoretical computation, the minimum disappears.²⁸ This may be the case for the pure and very diluted Cd samples. Figure 8 also indicates that for the less diluted Cd-Zn samples the "vertical" scattering might still occur below temperatures $T/\theta \approx 0.02$, which is rather low compared to where the dominance of this kind of scattering generally occurs ($T/\theta \approx 0.1$).

The Fermi sphere of Cd is intersected in many places by zone boundaries causing the Fermi surface to be highly fragmented. The usual description²⁹ of the Fermi surface results from translating the many pieces by the appropriate reciprocal lattice vectors. The resultant Fermi surface has two components which are of importance here.

First, the third-zone electron sheet (so-called "lens") is a disk-shaped closed surface having a symmetry axis parallel to [0001]. Second are the highly complicated second-zone hole sheets which have a symmetry axis and also an open direction along [0001].

In the case of a simple spherical surface, the probability of umklapp scattering decreases drastically at low temperatures because of the cutoff in the number of phonons with momentum vectors sufficiently large to make such processes possible. The high degree of fragmentation results in the availability of small-momentum phonons for producing umklapp scatterings from states close to the zone boundaries. This model was also used³⁰ for the explanation of extraordinary phonon-drag effects in the thermoelectric properties of copper. The almost spherical Fermi surface for Cu touches the zone boundary, and electrons in states on the belly not too far from the neck relax by umklapp scattering towards the points where the neck contacts the zone boundary. This implies the possibility of umklapp scattering by phonons having small \vec{q} values and varying continuously down to $\vec{q} \rightarrow 0$, in contrast to the case for simpler metals where the limiting $\vec{q} \neq 0$ stops umklapp processes at a relatively higher temperature.

If such processes were to occur in the case of Cd, then the rapid decrease of the thermal resistivity with temperature may be associated with the freezing out of umklapp scattering. The dimensions of the electron lens and hole surfaces indicate that the magnitude of the phonon momentum vector should be approximately $\frac{1}{5}q_0 - \frac{1}{3}q_0$, where q_0 is the Debye wave number, in order for appreciable umklapp scattering to occur. The quadratic temperature dependence for W_i , which has been observed for $T \approx 4$ K and below (Figs. 3 and 4), could mean that these extra umklapp processes are frozen out at the lowest temperatures for the particular specimen considered. The occurrence below 4 K of regions, where $W_i \propto T^2$ holds and expansion of this region with increasing Zn concentration to higher temperature, indicates that the presence of impurities decreases the probability for umklapp processes.

A comparison between thermal-conductivity data for metals having fragmented Fermi surfaces is rather summary because of the lack of systematic investigations on metals with properly chosen concentrations of impurities. A comparison is made by plotting $\log_{10}(W_i/W_\infty)$ vs $\log_{10}(T/\theta_0)$, as shown on Fig. 9, for several metals. Here W_∞ is the limiting value of W_i for large temperatures and θ_0 is the Debye temperature at 0 K. Data from several sources³¹⁻⁴³ are shown for Na, Cu, Ag, Al, In, Mg, and Hg as well as the present results for two dilute Cd-Zn alloys. The data for these alloys

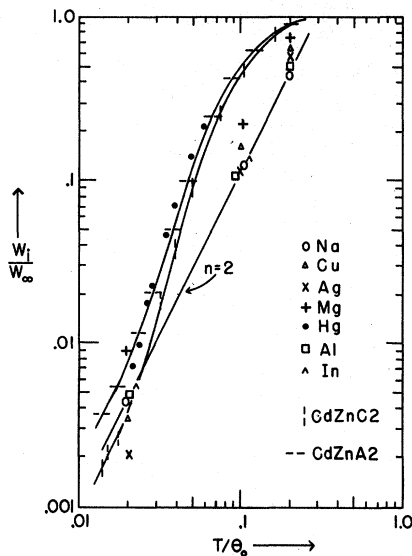


FIG. 9. Reduced intrinsic thermal resistivities as a function of reduced temperature for several metals.

have been plotted instead of those for the pure Cd since the alloys were measured for a larger number of temperatures, and, as can be seen from Figs. 3 and 4, the difference in W_i for Cd is negligible in the temperature range of interest (above $T/\theta_0 \approx 0.05$). It is seen that the data for Cd and also for Hg deviate markedly toward larger W_i/W_∞ values over most of the T/θ_0 range plotted. Data available¹ for Zn cannot be used since the impurity concentration is rather large.

The similarity of the two curves for Cd and Hg is striking. The rhombohedral structure of Hg leads to a Fermi surface that has large lens-shaped electron sheets outside the first zone in three crystallographic directions.⁴⁴ When across these lenses umklapp processes can occur in a manner similar to those in the case of the Fermi surface of Cd, the similarity of the two elements in their electronic thermal conduction properties relative to metals without such configurations seems to be plausible.

*Research supported by the National Science Foundation.

[†]Work part of the requirements for a Ph. D. degree. Present address: Southeastern Branch, University of Connecticut, Groton, Conn.

¹H. M. Rosenberg, *Phil. Mag.* **2**, 541 (1957).

²B. N. Aleksandrov and I. G. D'yakov, *Zh. Eksperim. i Teor. Fiz.* **43**, 852 (1962) [*Soviet Phys. JETP* **16**, 603 (1963)].

³S. B. Das and A. N. Gerritsen, *Phys. Rev.* **135**, 1081 (1964).

⁴O. P. Katyal and A. N. Gerritsen, *Phys. Rev.* **178**, 1037 (1969).

⁵Richard A. Young, J. Ruvalds, and L. M. Falicov,

SUMMARY

The results and conclusions for the intrinsic thermal resistivity W_i of Cd and Cd-Zn alloy crystals below 20 K can be summarized as follows:

(i) W_i deviates from $W_i \propto T^2$ for a temperature range that is largest, and with the most pronounced deviation, for the purest crystals.

(ii) Impurities and strain generate in W_i a term proportional to T^2 ; this term disappears at a temperature that is higher when the amount of Zn solute is larger. There is indication that for Zn concentrations of order 1 at. % the range for $W_i \propto T^2$ is continuous.

(iii) For the Zn concentrations investigated (below 0.56 at. %) there is practically no correlation between electron-phonon scattering and the non-Debye phonon spectrum, even in the lowest-temperature regions where a term $W_i \propto T^2$ exists. But the results indicate that this correlation may be realized over a large temperature range when the solute concentration is sufficiently large.

(iv) The anomalous behavior is strongly dependent on crystal anisotropy, even though for experimental reasons the measured dependence presents a qualitative relation only.

(v) The ratio of the thermal and electrical intrinsic resistivities suggests that umklapp scattering across parts of the Fermi surface may be important for those temperatures where W_i deviates from $W_i \propto T^2$. This umklapp scattering is a possible consequence of the high degree of fragmentation of the Fermi surface. This statement is supported by a qualitative agreement between the $W_i(T)$ curves for Cd and Hg.

ACKNOWLEDGMENTS

The authors are very much indebted to Professor H. J. Yearian for the crystallographic alignment of the crystal ingots before the samples were cut. Thanks are due to Dr. O. P. Katyal for making some of the electrical-resistivity measurements. Discussions with Professor P. G. Klemens were greatly appreciated.

Phys. Rev. **178**, 1048 (1969).

⁶O. P. Katyal and A. N. Gerritsen, *Phys. Rev.* **185**, 1017 (1969).

⁷Yu. Kagan and A. P. Zhernov, *Zh. Eksperim. i Teor. Fiz.* **50**, 1107 (1966) [*Soviet Phys. JETP* **23**, 737 (1966)].

⁸Harshaw Chemical Company, Midland, Mich.

⁹AREMCO Products Inc., Briarcliff Manor, N. Y.

¹⁰Battelle Memorial Institute, Columbus, Ohio.

¹¹SMC Servomet, Jarrel-Ash Co., Waltham, Mass.

¹²R. Bogaard, Ph. D. thesis, Purdue University, 1970 (unpublished).

¹³Cryocal Inc., Riviera Beach, Fla.

¹⁴Bleeker, Zeist, Holland.

¹⁵Type Zc, Kipp, Delft, Holland.

- ¹⁶Leeds and Northrup, student potentiometer.
- ¹⁷A. A. R. El Agib, *J. Sci. Instr.* **41**, 592 (1964).
- ¹⁸P. G. Klemens, in *Encyclopedia of Physics*, edited by S. Flügge (Springer-Verlag, Berlin, 1956), Vol. 14.
- ¹⁹R. H. Bogaard and A. N. Gerritsen, in *Thermal Conductivity*, edited by C. Y. Ho and R. E. Taylor (Plenum, New York, 1969), p. 185. The results presented in Figs. 2-4 contain those reported in this preliminary paper as well as the results of extended measurements to below 3 K with sample Cd C3 and a few alloys.
- ²⁰B. N. Aleksandrov, *Zh. Eksperim. i Teor. Fiz.* **43**, 399 (1962) [*Soviet Phys. JETP* **16**, 286 (1963)].
- ²¹P. Wyder, *Physik Kondensierten Materie* **3**, 263 (1965).
- ²²N. E. Phillips, *Phys. Rev.* **134**, 385 (1964).
- ²³P. L. Smith and N. M. Wolcott, *Phil. Mag.* **1**, 854 (1956).
- ²⁴R. S. Craig, C. A. Krier, L. W. Coffey, E. A. Bates, and W. E. Wallace, *J. Am. Chem. Soc.* **76**, 238 (1954).
- ²⁵C. W. Garland and J. Silverman, *Phys. Rev.* **119**, 1218 (1960).
- ²⁶M. Kohler, *Z. Physik* **126**, 495 (1949).
- ²⁷R. L. Powell, W. J. Hall, and H. M. Roder, *J. Appl. Phys.* **31**, 496 (1960).
- ²⁸For these and further considerations, see J. M. Ziman, *Electrons and Phonons* (Clarendon, Oxford, England, 1960), Chap. IX.
- ²⁹R. C. Jones, R. G. Goodrich, and L. M. Falicov, *Phys. Rev.* **174**, 672 (1968).
- ³⁰J. M. Ziman, *Phys. Rev.* **121**, 1320 (1961).
- ³¹R. L. Powell and W. A. Blanpied, *Natl. Bur. Std. (U.S.), Circ.* **556** (1954).
- ³²R. Berman and D. K. C. MacDonald, *Proc. Roy. Soc. (London)* **A209**, 368 (1951).
- ³³J. D. Filby and D. L. Martin, *Proc. Roy. Soc. (London)* **A276**, 187 (1963).
- ³⁴R. Berman and D. K. C. MacDonald, *Proc. Roy. Soc. (London)* **A211**, 122 (1952).
- ³⁵D. L. Martin, *Phys. Rev.* **141**, 576 (1966).
- ³⁶G. K. White, *Proc. Phys. Soc. (London)* **66A**, 844 (1953).
- ³⁷F. A. Andrews, R. T. Webber, and D. A. Spohr, *Phys. Rev.* **84**, 994 (1951).
- ³⁸W. T. Berg, *Phys. Rev.* **167**, 583 (1968).
- ³⁹R. E. Jones and A. M. Toxen, *Phys. Rev.* **120**, 1167 (1960).
- ⁴⁰C. A. Bryant and P. H. Keesom, *Phys. Rev.* **123**, 491 (1961).
- ⁴¹R. T. Webber and D. H. Spohr, *Phys. Rev.* **106**, 927 (1957).
- ⁴²B. Van der Hoeven and P. H. Keesom, *Phys. Rev.* **135**, 631 (1964).
- ⁴³J. A. Rayne, *J. Phys. Chem. Solids* **7**, 268 (1958).
- ⁴⁴J. M. Dishman and J. A. Rayne, *Phys. Rev.* **166**, 728 (1968).

Calorimetric Determination of the Density of Electronic States in α -Phase Indium Alloys. I. Alloys with Tin[†]

Marcel H. Lambert,* J. C. F. Brock,† and Norman E. Phillips
*Inorganic Materials Research Division of the Lawrence Radiation Laboratory and
 Department of Chemistry, University of California, Berkeley, California 94720*
 (Received 11 September 1970)

The low-temperature heat capacity of each of a series of indium-tin alloys containing 0-13 at. % tin has been measured, and the density of electronic states $N(E_F)$ and the Debye temperature Θ_0 evaluated. The electron-phonon coupling constant λ was calculated from the superconducting critical temperature T_c and Θ_0 , and was used to derive the band-structure density of states $N_{bs}(E_F)$. Both $N_{bs}(E_F)$ and λ increase more rapidly with increasing tin content above 9 at. % tin than below 9 at. %. These results are interpreted in terms of the Brillouin-zone-boundary-Fermi-surface interaction that has been postulated to explain the behavior of the lattice parameters and T_c . Comparison with band-structure calculations and experimental Fermi-surface studies for pure indium suggest that new parts of the Fermi surface appear in the third zone at this electron concentration.

I. INTRODUCTION

In recent years, a variety of elegant techniques for determining the geometry of the Fermi surface have been applied to pure metals, and the shape of the Fermi surface is now known in considerable detail for many of them. The addition of an alloying metal changes the Fermi surface by changing the conduction-electron/atom ratio Z , and also through

the effect of the different ion-core potential on the energy-momentum relation of the conduction electrons. Unfortunately, the techniques that have made the most important contributions to the determination of the Fermi-surface geometry of pure metals require long electron mean free paths and are therefore not applicable to alloys. As a consequence, very little is known about the changes in the Fermi surface that accompany alloying. Of the